CrystEngComm

ROYAL SOCIETY OF CHEMISTRY

PAPER

View Article Online
View Journal | View Issue



Cite this: *CrystEngComm*, 2023, **25**, 5316

# Chalcogen bonding interactions in a series of aromatic selenocyanates†

Jan Alfuth, [ab] Olivier Jeannin [a] and Marc Fourmigué *[a]

Received 26th July 2023,
Accepted 30th August 2023

DOI: 10.1039/d3ce00745f

rsc.li/crystengcomm

Selenium atoms in *aromatic* selenocyanates are characterized by the occurrence of two σ-holes, a stronger one in the prolongation of the NC–Se bond and a weaker one in the prolongation of the Ar–Se bond. The crystal structures of several bis(selenocyanato) derivatives, prepared by a method originally developed for *ortho* bis-substituted derivatives, illustrate very well this difference, with a short NC–Se···NC ChB interaction organizing the molecules into 1D motifs with reduction ratio (RR) values in the range of 0.87–0.91 (RR is defined as the interatomic distance over the van der Waals contact), complemented with Ar–Se···NC ChB interactions between antiparallel chains involving the second σ-hole, with larger RR values in the range of 0.92–0.94. Comparison with *benzylic* selenocyanates shows that this secondary lateral interaction involving the weaker σ-hole is notably enhanced in these novel *aromatic* compounds. The structure of co-crystals of the *para* derivative (1,4-diselenocyanatobenzene) with (*E*)-1,2-di(4-pyridyl)ethylene (**bpen**) is characterized by an extremely short NC–Se···$N_{bpen}$ distance at 2.693(2) Å, *i.e.* a RR value of 0.78, complemented with interaction of the second σ-hole with the π system of the double bond of **bpen**.



## Introduction

Following the intense efforts of the last thirty years conducted on the investigation of halogen bonding in crystal engineering strategies,[1,2] this prototypical σ-hole interaction has by now been found in many other groups of the entire periodic table,[3] and particularly in the closely related group 16 of the chalcogens.[4] Chalcogen bonding has been accordingly defined as the interaction between a positively polarized chalcogen atom and a Lewis-base (LB)[5] and has been the subject of several review papers in the recent years.[6] Many reported systems are based on self-complementary molecules, *i.e.* molecules bearing simultaneously a chalcogen bond (ChB) donor and a ChB acceptor groups, as illustrated in Scheme 1.[7–9]

Among them, organic selenocyanates (Scheme 1c) have been shown to provide a recurrent one-dimensional infinite motif where the strongly activated σ-hole in the prolongation of the NC–Se bond interacts with the nitrogen lone pair of a neighbouring molecule.[10] Extensive series of *benzylic* selenocyanates, with one or several SeCN groups, have been reported because of their ease of preparation from the corresponding benzyl halides.[11] On the other hand, the number of *aromatic* selenocyanates is more limited, and restricted essentially to mono selenocyanate derivatives.[12] We have recently developed a synthetic procedure toward aromatic bis(selenocyanate) derivatives[13] and shown that the

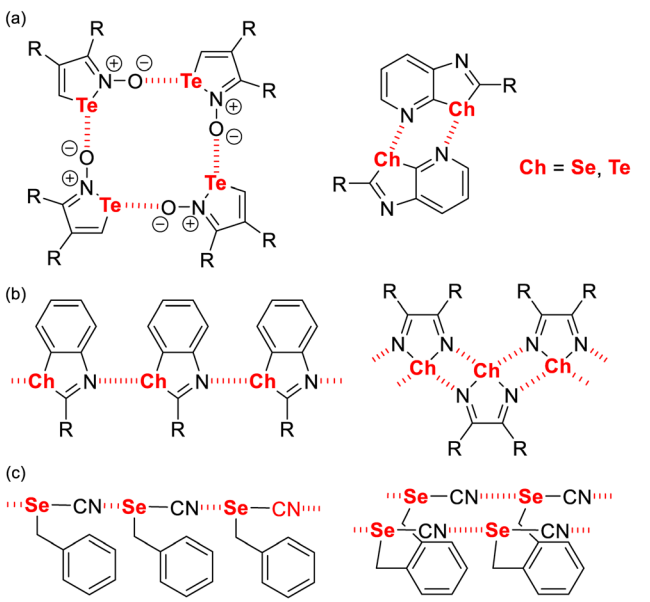


**Scheme 1** Examples of self-associated ChB donors into (a) cyclic motifs, (b and c) infinite 1D motifs.

[a] *Université de Rennes, CNRS, ISCR (Institut des Sciences Chimiques de Rennes) UMR 6226, 35000 Rennes, France. E-mail: marc.fourmigue@univ-rennes.fr*
[b] *Department of Organic Chemistry, Gdańsk University of Technology, 80-233 Gdańsk, Poland*

† Electronic supplementary information (ESI) available: Fig. S1 and S2, details on theoretical calculations and crystallographic data. CCDC 2280515–2280520. For ESI and crystallographic data in CIF or other electronic format see DOI: https://doi.org/10.1039/d3ce00745f

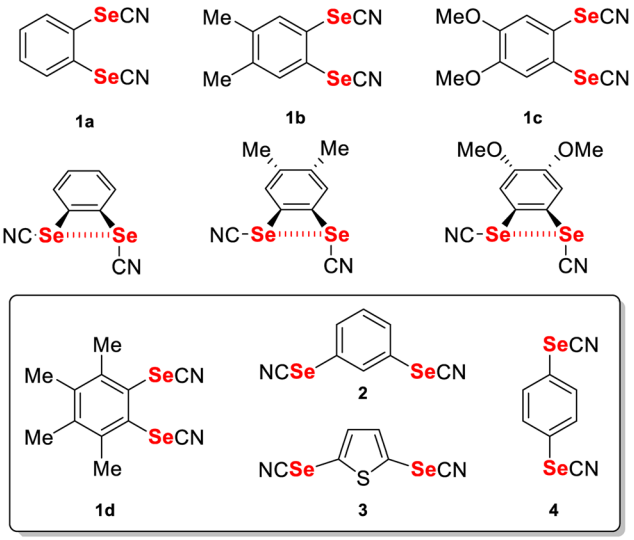


**Scheme 2** Known *ortho* bis(selenocyanate) derivatives and the target compounds **1d**, **2**–**4**.

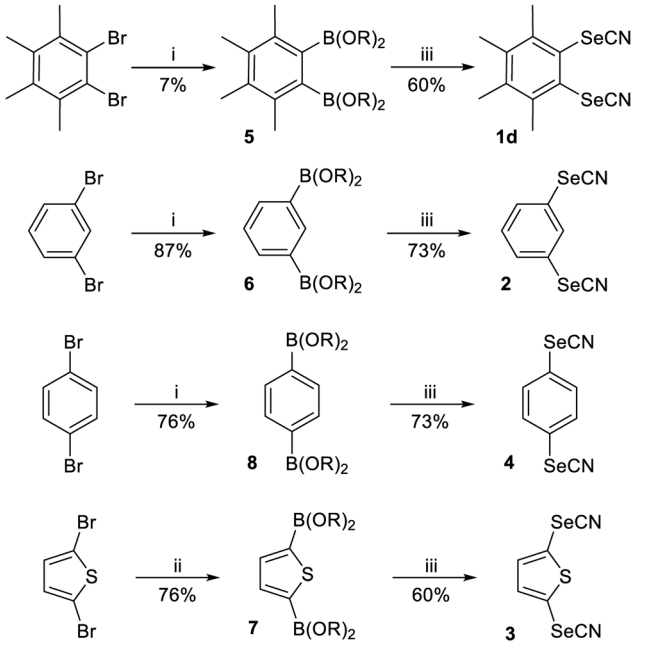


**Scheme 3** Synthetic path to **1d**, **2**–**4**. i: bis(pinacolato)diborane, KOAc, $[(dppf)PdCl_2]_{cat}$ in DMF, 80 °C, 16 h; ii: bis(pinacolato)diborane, KOAc, $[Pd(PPh_3)_4]_{cat}$ in dioxane, 90 °C, 48 h; iii: $SeO_2$, malononitrile in DMSO, 60 °C, 16 h.

*ortho*-substituted bis(selenocyanato)benzene derivatives such as **1a–c** (Scheme 2) crystallise with an intramolecular NC–Se···Se ChB. Co-crystallization with (*E*)-1,2-di(4-pyridyl) ethylene (**bpen**) led to the formation of rectangular motifs stabilized by NC–Se···$N_{bpen}$ chalcogen bonding interactions, where the face-to-face association of **bpen** molecules favoured their photocyclization to cyclobutane adducts through single-crystal-to-single-crystal [2 + 2] photodimerization. In this paper, we want to extend further the crystal chemistry of such bis(selenocyanato)benzene derivatives to the more sterically constrained *ortho* derivative (**1d**) as well as to the *meta* (**2**, **3**) and *para* (**4**) analogues. In all these situations where the *intramolecular* ChB is not possible anymore, the crystal structures reveal the effects of the presence of two sizeable σ-holes on each selenium atom, both able to participate in ChB interactions, as demonstrated below. Furthermore, cocrystals of both **2** and **4** with **bpen** were also obtained and analysed, showing particularly strong NC–Se···$N_{bpen}$ chalcogen bonds.

## Results and discussion

### Syntheses

The preparation of simple aromatic selenocyanates is usually based on the reaction of KSeCN with either diazonium salts[14] or more electrophilic diaryliodonium salts,[15] as reported for *para*-substituted derivative **4**.[12c,16] It has been recently reported that the *ipso*-functionalization of arylboronic acids affords arylselenocyanates in good yields, using either Se powder with TMS–CN,[17] or $SeO_2$ and malononitrile.[18] We have recently adapted the last procedure, originally reported only for *mono* boronic acids,[19] for the preparation of disubstituted *ortho*-bis(selenocyanato)benzene derivatives **1a–c** by performing the selenocyanation reaction directly on boronic esters such as the *ortho*-bis(pinacol) boranes.[13] As shown in Scheme 3, we have here extended this procedure with four other dibromoaromatic derivatives, which have been transformed through a Miyaura borylation reaction with bis(pinacolato)diborane to give the four corresponding bis(pinacol) boranes **5–8** in 76-87% yields, except with the sterically congested *ortho*-dibromotetramethylbenzene (7% yield). The following selenocyanation reactions of **5–8** with $SeO_2$ and malononitrile successfully afforded **1d** and **2–4** in 60–73% yields.

### Electrostatic surface potentials

The ChB donor ability of **1d**, **2–4** has been first evaluated based on the calculated values of the extrema of the electrostatic potential (ESP) surfaces – the larger the positive ESP value, the more important the σ-hole at the chalcogen atom and therefore the ChB donor ability. As shown in Fig. 1 (see calculation details in ESI†), two σ-holes are systematically observed on the Se atoms, the strongest one in the prolongation of the NC–Se bond, the weaker one in the prolongation of the $C_{Ar}$–Se bond. Notable differences are observed between the four compounds. In the sterically constrained tetramethyl benzene derivative **1d**, one SeCN moiety partly interacts with the neighbouring Se atom, leading to decreased $V_{S,max}$ values ($V_{S,max}$ is the most positive surface electrostatic potential). On the other hand, in both *meta* and *para* derivatives **2** and **4**, geometry optimization afforded planar structures with the SeCN moieties lying within the aromatic plane. Under these circumstances, the strongest σ-hole on the Se atoms merges with the electron-

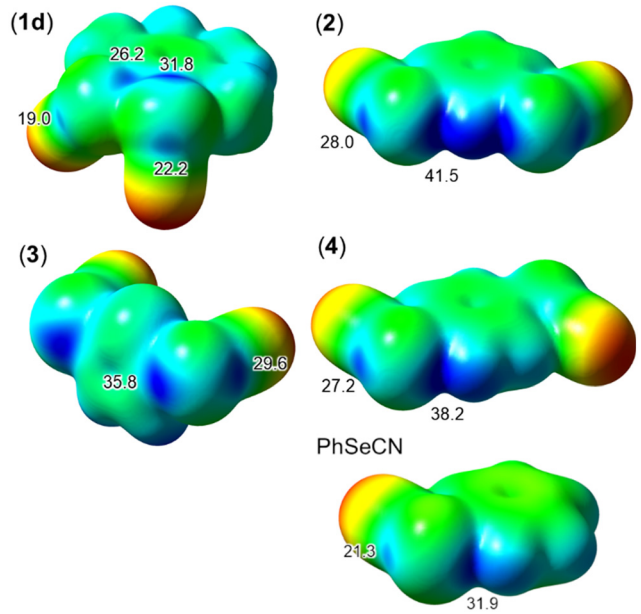


Fig. 1 Computed electrostatic potential on the 0.002 au isodensity surface of **1d**, **2**–**4** and the model compound PhSeCN. Potential scale ranges from −37.7 kcal mol$^{-1}$ (in red) to +43.9 kcal mol$^{-1}$ (in blue). $V_{S,max}$ values for the two σ-holes (in blue) on the selenium atoms are calculated on the 0.001 au isodensity surface and are given in kcal mol$^{-1}$.

depleted area of the neighbouring aromatic H atom, leading to an overall enhancement of the strongest $V_{S,max}$ values up to 41.5 and 38.2 kcal mol$^{-1}$ in **2** and **4**, respectively. The situation differs in the thiophene derivative **3** where the SeCN moieties are rotated out of the aromatic plane. In that respect, the $V_{S,max}$ values found in **3** are representative of a SeCN moiety with limited interaction with the aromatic system. A specific feature here is the proximity of the $V_{S,max}$ values of both σ-holes, at 35.8 kcal mol$^{-1}$ along the NC–Se bond and 29.6 kcal mol$^{-1}$ along the $C_{Ar}$–Se bond. Also, comparison with the mono-substituted phenyl selenocyanate shows that the disubstitution (as in **2** and **4**) increases both σ-holes on the Se atoms.

A striking difference with the extensive series of *benzylic* selenocyanates reported to date is the strength of this second σ-hole, which differs from the strongest one by only 10 kcal mol$^{-1}$, while a 20 kcal mol$^{-1}$ difference was recurrently observed in the *benzylic* selenocyanates.[10] The question then arises if the directing effect of the strongest σ-hole, clearly identified in the structures of *benzylic* selenocyanates to favour ···NC–(R)Se···NC–(R)Se··· chain-like motifs,[10,11] will be maintained in these aromatic systems.

## Crystal structures

Tetramethyl-1,2-bis(selenocyanato)benzene **1d** crystallizes in the monoclinic system, space group $P2_1/c$, with two crystallographically independent molecules, both in general position. At variance with the other reported *ortho*-bis(selenocyanato)benzene derivatives **1a–c**, the methyl

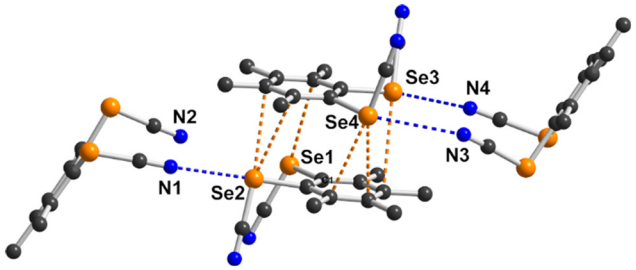


Fig. 2 Details of the ChB interactions in **1d**. ChBs in the prolongation of the NC–Se bonds are indicated as orange dotted lines, those in the prolongation of the $C_{Ar}$–Se bonds as blue dotted lines.

substitution α to the SeCN moieties hinders the planarization of one of these groups and the formation of an intramolecular ChB illustrated in Scheme 2. Indeed, as shown in Fig. 2, the two SeCN groups of each molecule point now out of the benzene ring, with the Se atoms interacting with the electron-rich π system of the other independent molecule, forming dimeric entities with short NC–Se···$C_{Ar}$ bonds. Structural characteristics of these ChB are collected in Table 1. Other ChB interactions can be identified between the dyads, involving the secondary σ-hole of the Se atoms, and the nitrogen atoms of neighbouring dyads. Surprisingly, these interactions involving the weaker σ-hole of the Se atoms are quite short with the Se2···N1 distance for example at 3.149(5) Å, *i.e.* a reduction ratio (RR) value of 0.91.

The structures of compounds **2** and **3** are very closely related. They both crystallize in the orthorhombic system, space group *Pnma*, with the molecule containing a crystallographic mirror plane and the SeCN groups pointing out of the aromatic plane, with a torsion angle of 73° in **2** and 57° in **3**. As shown in Fig. 3 for the compound **3** (*cf.* Fig. S1† for **2**), the shortest ChB involves the strongest σ-hole in the prolongation of the NC–Se bond, leading to very short Se···N distances, 3.128(7) and 3.045(2) Å in **2** and **3**, respectively, *i.e.* RR values of 0.91 and 0.88, and leading to the formation of chain motifs running along the *a* axis. Lateral $C_{Ar}$–Se···N ChB interactions between chains involve the second σ-hole and are only slightly longer (Table 2).

Table 1 Structural characteristics of ChBs in **1d**. The RR values are calculated on the basis of Bondi's van der Waals radii, giving contact distances of Se···C 3.60 Å and Se···N 3.45 Å

| ChB | ChB dist. (Å) | RR | ChB ang (°) |
|---|---|---|---|
| NC–Se1···C18 | 3.583(5) | 0.99 | 154.04(12) |
| NC–Se2···C15 | 3.516(6) | 0.98 | 148.40(12) |
| NC–Se2···C16 | 3.379(4) | 0.94 | 165.43(12) |
| NC–Se3···C5 | 3.630(4) | 1.00 | 168.57(12) |
| NC–Se4···C3 | 3.475(6) | 0.96 | 172.75(12) |
| NC–Se4···C4 | 3.391(4) | 0.94 | 157.03(12) |
| $C_{Ar}$–Se2···N1$^{i}$ | 3.149(5) | 0.91 | 172.71(12) |
| $C_{Ar}$–Se3···N4$^{ii}$ | 3.199(4) | 0.93 | 164.95(12) |
| $C_{Ar}$–Se4···N3$^{ii}$ | 3.510(7) | 1.02 | 140.89(11) |

$^{i}$ $-x$, $0.5 + y$, $0.5 - z$, $^{ii}$ $1 - x$, $-0.5 + y$, $1.5 - z$.

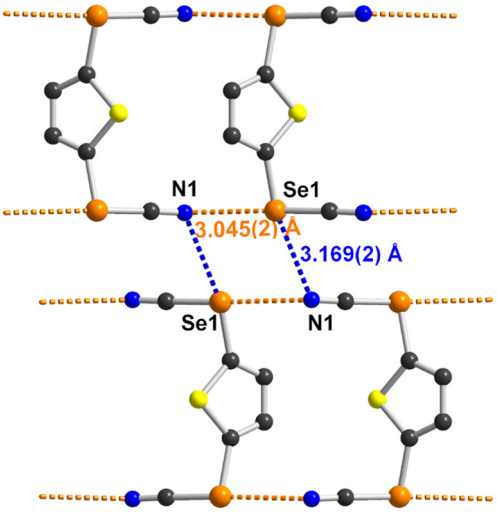


Fig. 3 Details of the solid-state organization for **3**. ChBs in the prolongation of the NC–Se bonds are indicated as orange dotted lines, those in the prolongation of the $C_{Ar}$–Se bond as blue dotted lines.

Table 2 Structural characteristics of ChB interactions in **2** and **3**. The RR values are calculated on Se···N contact distances of 3.45 Å

| Compound | ChB | ChB dist. (Å) | RR | ChB ang (°) |
|---|---|---|---|---|
| **2** | NC–Se1···N1$^{i}$ | 3.128(7) | 0.91 | 168.36(29) |
| | $C_{Ar}$–Se1···N1$^{ii}$ | 3.223(7) | 0.93 | 173.37(25) |
| **3** | NC–Se1···N1$^{i}$ | 3.045(2) | 0.88 | 175.52(6) |
| | $C_{Ar}$–Se1···N1$^{ii}$ | 3.169(2) | 0.92 | 167.12(6) |
| **4** | NC–Se1···N1$^{iii}$ | 3.060(2) | 0.87 | 176.09(7) |
| | $C_{Ar}$–Se1···N1$^{iv}$ | 3.229(6) | 0.94 | 167.33(6) |

$^{i}$ 0.5 + *x*, *y*, 1.5 − *z*, $^{ii}$ 0.5 − *x*, 1 − *y*, −0.5 + *z*, $^{iii}$ *x*, 0.5 − *y*, 0.5 + *z*, $^{iv}$ −*x*, −0.5 + *y*, 0.5 − *z*.

The structure of the *para*-substituted compound **4** has been already reported in the literature[12c] and has been redetermined here, improving significantly the precision on bond distances and angles (Fig. 4). It crystallizes in the monoclinic system, space group $P2_1/c$, with one independent molecule located on inversion centre. At variance with the structure optimization in gas phase (see above in Fig. 1), the SeCN moieties are not coplanar with the aromatic ring but make an angle of 43°. As shown in Fig. 4, the Se atom participates in two ChB interactions, the strongest one in the prolongation of the NC–Se bond and the weaker but sizeable one in the prolongation of the $C_{Ar}$–Se bond (*cf.* Table 2).

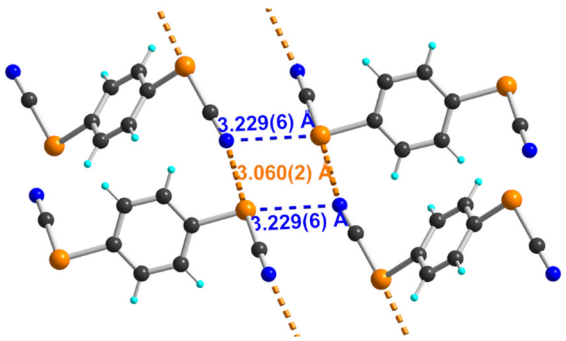


Fig. 4 Details of the solid-state organization for **4**. ChBs in the prolongation of the NC–Se bonds are indicated as orange dotted lines, those in the prolongation of the $C_{Ar}$–Se bond as blue dotted lines.

It is interesting at this stage to compare the systems described here with other aromatic selenocyanates as well as the extensive series of *benzylic* selenocyanates reported earlier. We have collected in Table 3 the structural characteristics of aromatic selenocyanates reported in the literature, excluding those exhibiting intramolecular ChB. In all derivatives as well as in **2**–**4**, the strongest ChB involves the σ-hole in the prolongation of the NC–Se bond, while the secondary $C_{Ar}$–Se···N interaction along the $C_{Ar}$–Se bond is weaker (RR = 0.91–1.02) but most often below the van der Waals contact distance, particularly in **2**–**4** (RR = 0.92–0.93). These observations confirm the analysis of the ESP maps and the correlation between the values of the $V_{S,max}$ extrema and the strength of the ChB interactions associated with the Se···N distance. This point is further illustrated by the comparison with *benzylic* selenocyanates. They are characterized indeed by a comparable σ-hole in the prolongation of the NC–Se bond but a notably weaker σ-hole in the prolongation of the $ArCH_2$–Se bond.[10] As a consequence, this secondary $ArCH_2$–Se···N interaction has been rarely mentioned, and when present, is observed at much longer distances, above the van der Waals contact distances (3.45 Å). This point is illustrated in Fig. 5 where the structures of the simplest phenyl selenocyanate and benzyl selenocyanate are compared.

### Adducts with 1,2-bis(4-pyridyl)ethylene (bpen)

The **bpen** adducts with the *ortho* derivatives **1a**–**c** have been reported to form tetramolecular associations into rectangular boxes with a short face-to-face interaction between **bpen** molecules, allowing for [2 + 2] cycloaddition under UV irradiation.[13] We considered similar co-crystallization experiments of **1d**, **2**, **3** and **4** with **bpen** but could obtain co-crystals only with **2** and **4**, as described below.

The *meta* derivative **2** co-crystallizes with **bpen** in the triclinic system, space group $P\bar{1}$, with one molecule **2** in general position, one **bpen** molecule disordered on two positions on an inversion centre and one **bpen** molecule, also located on an inversion centre, but with 0.5 occupancy (Fig. 6, see also Fig. S2† for disorder model). This corresponds to a $(\mathbf{2})_2(\mathbf{bpen}\_A)(\mathbf{bpen}\_B)_{0.5}$ complex formulation. Molecule **bpen**_B is not engaged in ChB interactions while molecule **bpen**_A interacts primarily with two molecules of **2** through two short NC–Se1···N3A [2.97(1) Å, RR = 0.86] and NC–Se1···N3B [3.03(1) Å, RR = 0.88] chalcogen bonds. The second σ-hole on Se1 as well as the two σ-holes on Se2 interact with nitrogen atoms of neighbouring molecules with slightly weaker interactions (Table 4). The overall structure does not

**Table 3** Details of the ChB interactions around selenium atom in structurally characterized aromatic selenocyanates (excluding those exhibiting intramolecular ChB)

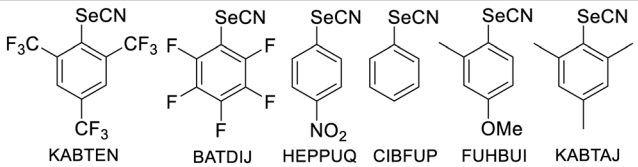


| | Along NC–Se bond | | Along $C_{Ar}$–Se bond | | |
|---|---|---|---|---|---|
| Compound | Interaction | RR | Interaction | RR | Ref. |
| KABTEN[i] | Se···N | 0.83 | Se···N | 0.91 | 12*d* |
| | Se···N | 0.86 | — | — | |
| BATDIJ | Se···N | 0.86 | Se···N | 1.00 | 12*b* |
| HEPPUQ | Se···O | 0.96 | Se···N | 0.97 | 20 |
| CIBFUP | Se···N | 0.89 | Se···N | 0.96 | 12*a* |
| FUHBUI | Se···O | 0.94 | Se···N | 1.00 | 21 |
| KABTAJ | Se···$(C_6)$[ii] | 0.95 | Se···N | 1.02 | 12*d* |

[i]Two crystallographically independent molecules in the unit cell. [ii]$C_6$: centroid of the benzene ring.

lead to a face-to face organization of **bpen** molecules which could favour [2 + 2] cycloadditions.

The adduct of the *para* derivative **4** with **bpen** crystallizes in the monoclinic system, space group $P2_1/c$, with both **4** and **bpen** on inversion centre, corresponding to a 1 : 1 stoichiometry (Fig. 7). As in the structure of compound **4** alone (see above), the SeCN moieties are not coplanar with the aromatic ring but make an angle of 47°. A chain-like motif is formed through the interaction of the stronger σ-hole of the Se atom with the pyridinic nitrogen atom, at an extremely short distance of 2.693(2) Å, *i.e.* a RR value of 0.78. The second σ-hole of the Se atom is engaged in a weaker but directional interaction with the π cloud of the central double bond of a neighbouring **bpen** molecule, with the shortest Se···$C_\pi$ distance at 3.531(7) Å, *i.e.* a RR value of 0.98, with a $C_{Ar}$–Se1···$C_\pi$ angle at 165.49(6)°. Here again, the solid-state organization does not favour [2 + 2] cycloaddition.

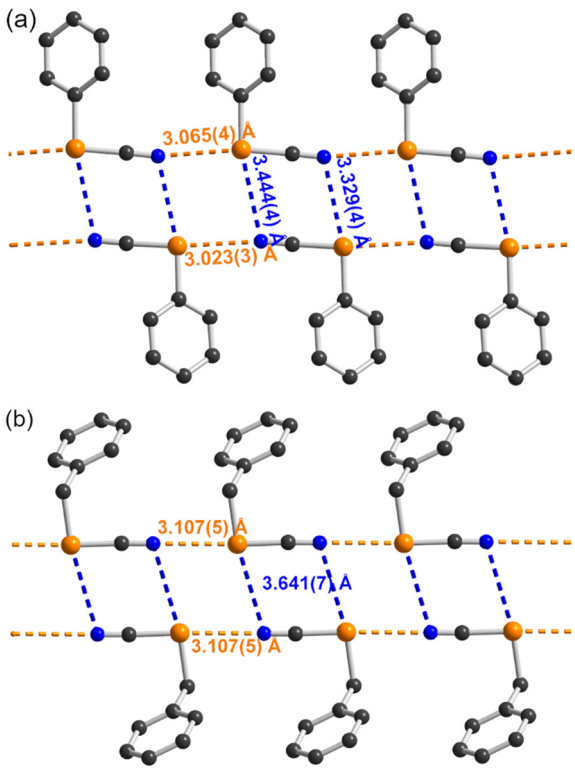


**Fig. 5** Comparison of the ChB interactions between (a) the *aromatic* PhSeCN selenocyanate (CCDC: CIBFUP)[12a] and (b) the *benzylic* BzSeCN selenocyanate (CCDC: CIGGOO).[11b] ChBs in the prolongation of the NC–Se bonds are indicated as orange dotted lines, those in the prolongation of the $C_{Ar}$–Se bond as blue dotted lines.

## Conclusions

We have demonstrated here that the synthetic access to bis(selenocyanato)benzene derivatives, reported earlier for *ortho*-substituted compounds, could be successfully extended to *meta* (**2**) and *para* (**4**) derivatives as well as the α,α′-disubstituted thiophene analogue **3**. Electrostatic potential (ESP) calculations show that selenium atoms in such *aromatic* selenocyanates are characterized by the occurrence of two

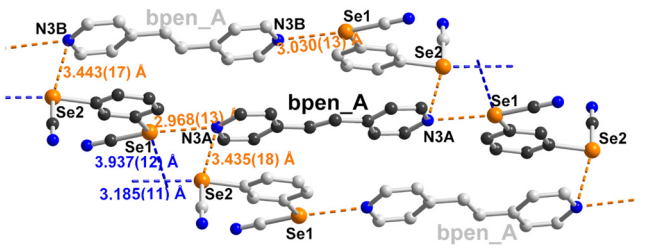


**Fig. 6** Details of the ChB interaction in $(\mathbf{2})_2$(**bpen**_A)(**bpen**_B)$_{0.5}$. Molecule **bpen**_B is not shown. Molecule **bpen**_A is disordered on inversion centre and only one of the two components is shown (black C atoms with N3A, grey C atoms with N3B). ChB interactions in the prolongation of the (NC)–Se bonds are indicated as orange dotted lines, those in the prolongation of the $C_{Ar}$–Se bond as blue dotted lines.

 

**Table 4** Structural characteristics of ChB interactions in (**2**)$_2$(**bpen**_A)(**bpen**_B)$_{0.5}$. The RR values are calculated on Se···N contact distances of 3.45 Å

| ChB | ChB dist. (Å) | RR | ChB ang (°) |
|---|---|---|---|
| NC–Se1···N3A$^{i}$ | 2.968(13) | 0.86 | 165.9(2) |
| NC–Se1···N3B$^{i}$ | 3.030(13) | 0.88 | 169.2(2) |
| $C_{Ar}$–Se1···N2$^{ii}$ | 3.937(12) | 1.14 | 162.13(8) |
| NC–Se2···N3A$^{iii}$ | 3.435(18) | 0.99 | 168.0(2) |
| NC–Se2···N3B$^{iii}$ | 3.443(17) | 1.00 | 166.1(2) |
| $C_{Ar}$–Se2···N1$^{iv}$ | 3.185(11) | 0.92 | 168.16(8) |

$^{i}$ $-1+x, -1+y, z$. $^{ii}$ $1-x, -y, -z$. $^{iii}$ $x, -1+y, z$. $^{iv}$ $2-x, -y, -z$.

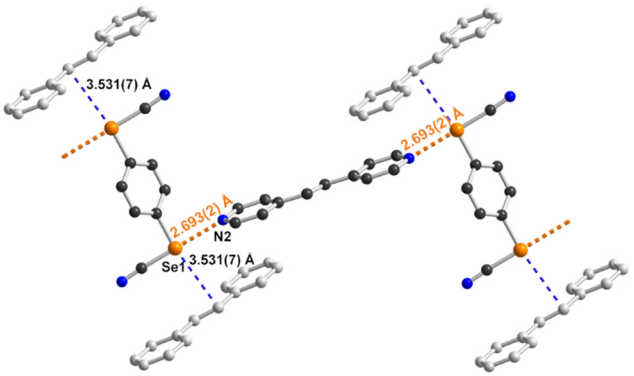


**Fig. 7** Details of the chain-like motif in the (**4**)(**bpen**) co-crystal.

σ-holes, a stronger one in the prolongation of the NC–Se bond and a weaker one in the prolongation of the Ar–Se bond. Their crystal structures illustrate very well this difference, with a short NC–Se···NC ChB interaction organizing the molecules into 1D motifs (RR values in the range of 0.87–0.91), complemented with Ar–Se···NC ChB interactions between antiparallel chains involving the second σ-hole, with larger RR values in the range of 0.92–0.94. On the other hand, in the sterically constrained tetramethyl-1,2-bis(selenocyanato)benzene *ortho*-derivative **1d**, an intramolecular ChB interaction is not possible (at variance the other *ortho*-bis-selenocyanates reported earlier) and both strong σ-holes in the prolongation of the two NC–Se bonds point toward the electron-rich π-cloud of a neighbouring molecule acting here as ChB acceptor. Comparison with *benzylic* selenocyanates shows that the secondary lateral interaction involving the weaker σ-hole is notably enhanced in the *aromatic* derivatives. Co-crystals of the *para* derivative **4** with **bpen** is characterized by an extremely short NC–Se···$N_{bpen}$ distance at 2.693(2) Å, *i.e.* a RR value of 0.78, complemented with interaction of the second σ-hole with the π system of the double bond of **bpen** acting here also as ChB acceptor. Further developments will involve the elaboration of 1,3,5-trisubstituted derivatives and their co-crystals, with neutral as well as anionic (halides) Lewis bases acceptors, expanding this even broader series of ChB systems based on such selenocyanates derivatives.

# Experimental section

## General considerations

Oxygen- and moisture-sensitive experiments were carried out under a dry oxygen-free argon atmosphere using standard Schlenk techniques. Solvents were dried by standard methods. The NMR spectra were recorded on Bruker spectrometers (300 MHz) referenced to residual solvent signals as internal standards. Elemental analyses were performed at Centre Regional de Mesures Physiques de l'Ouest (CRMPO) with Elementar Vario/Perkin Elmer 2400 series. (*E*)-1,2-di(4-pyridyl)ethylene (**bpen**) was obtained from Aldrich and used as received.

## General procedure for the Miyaura borylation reactions (derivatives 5, 6, 8)

To bis(pinacolato)diborane (635 mg, 2.5 mmol), anhydrous potassium acetate (589 mg, 6 mmol) and a dibromo derivative (1 mmol), 3.5 ml of anhydrous DMF was added and the mixture was degassed with argon. [1,1′-Bis(diphenylphosphino)ferrocene]palladium(II) dichloride (73 mg, 0.1 mmol) was added and the mixture was stirred in argon atmosphere at 80 °C overnight. After cooling to room temperature, the mixture was poured to a separatory funnel, diluted with water and extracted with AcOEt (50 ml). The aqueous layer was discarded and the organic layer was washed with water (twice) and brine and then dried over $MgSO_4$. Volatiles were removed on a rotovap and the crude product was purified by flash chromatography (petroleum ether : AcOEt = 9 : 1) to give pure diboronic acid pinacol diesters **5**, **6** and **8**.

**Compound 5.** Yield: 7%. White solid. $^{1}$H NMR (300 MHz, $CDCl_3$): $\delta$ 2.39 (s, 6H), 2.20 (s, 6H), 1.40 (s, 24H). $^{11}$B NMR (96 MHz, $CDCl_3$): $\delta$ 31.51.

**Compound 6.** Yield: 87%. White solid. $^{1}$H NMR (300 MHz, $CDCl_3$): $\delta$ 8.31 (td, $J$ = 1.4, 0.7 Hz, 1H), 7.93 (dd, $J$ = 7.4, 1.4 Hz, 2H), 7.40 (td, $J$ = 7.4, 0.8 Hz, 1H), 1.37 (s, 24H). $^{11}$B NMR (96 MHz, $CDCl_3$): $\delta$ 31.08. $^{13}$C NMR (75 MHz, $CDCl_3$): $\delta$ 141.24, 137.63, 127.03, 83.72, 24.87.

**Compound 8.** Yield: 76%. White solid. $^{1}$H NMR (300 MHz, $CDCl_3$): $\delta$ 7.83 (s, 4H), 1.37 (s, 24H). $^{11}$B NMR (96 MHz, $CDCl_3$): $\delta$ 32.09. $^{13}$C NMR (75 MHz, $CDCl_3$): $\delta$ 133.88, 83.82, 24.87.

**Compound 7.** To bis(pinacolato)diborane (635 mg, 2.5 mmol), anhydrous potassium acetate (589 mg, 6 mmol) and 2,5-dibromothiophene (242 mg, 1 mmol) 3.5 ml of anhydrous dioxane was added and the mixture was degassed with argon. Tetrakis(triphenylphosphine)palladium(0) (58 mg, 0.05 mmol) was added and the mixture was stirred in argon atmosphere at 90 °C for 48 h. After cooling to room temperature, the mixture was diluted with DCM and filtered through celite. Solvents were removed on a rotovap and the crude product was purified by flash chromatography (petroleum ether : DCM = 1 : 1) to give pure **7**. Yield: 76%. White solid. $^{1}$H NMR (300 MHz, $CDCl_3$): $\delta$ 7.69 (s, 2H), 1.36

(s, 24H). $^{11}$B NMR (96 MHz, $CDCl_3$): $\delta$ 28.96. $^{13}$C NMR (75 MHz, $CDCl_3$): $\delta$ 137.64, 84.10, 24.75.

### General procedure for the synthesis of the diselenocyanatoarenes[18]

To $SeO_2$ (666 mg, 6 mmol) and malononitrile (132 mg, 2 mmol) 2 ml of anhydrous DMSO was added in argon atmosphere and the mixture was stirred for 30 min at room temperature. To the resulting orange solution diboronic acid pinacol diester **5–8** (1 mmol) was added and the mixture was stirred at 60 °C overnight. After cooling to room temperature water (10 ml) was added and the mixture was extracted with DCM (3 × 20 ml). The organic layers were combined, dried with $MgSO_4$ and volatiles were removed on a rotovap. The crude product was purified by column chromatography (petroleum ether : DCM = 1 : 1 or petroleum ether : AcOEt = 9 : 1) to give pure diselenocyanatoarenes **1d**, **2–4**.

**Compound 1d.** Yield: 60%. Pale yellow needles, mp 150–151 °C. $^1$H NMR (300 MHz, DMSO-$d_6$): $\delta$ 2.66 (s, 6H), 2.31 (s, 6H). $^{13}$C NMR (75 MHz, DMSO-$d_6$): $\delta$ 139.91, 139.88, 131.78, 105.54, 24.13, 18.34. $^{77}$Se NMR (76 MHz, DMSO-$d_6$): $\delta$ 335.86. Elem. Anal. Calcd. for $C_{12}H_{12}N_2Se_2$: C, 42.12; H, 3.54; N, 8.19. Found: C, 41.84; H, 3.37; N, 8.09. Crystals for X-ray diffraction were obtained as pale yellow needles after dissolution in small amount of hot AcOEt and slow cooling to RT and layering with petroleum ether.

**Compound 2.** Yield: 73%. Light yellow solid, mp 89–90 °C. $^1$H NMR (300 MHz, DMSO-$d_6$): $\delta$ 8.06 (t, $J$ = 1.7 Hz, 1H), 7.80 (dd, $J$ = 7.9, 1.8 Hz, 2H), 7.52 (dd, $J$ = 8.3, 7.5 Hz, 1H). $^{13}$C NMR (75 MHz, DMSO-$d_6$): $\delta$ 137.35, 134.23, 131.96, 126.44, 105.55. $^{77}$Se NMR (76 MHz, DMSO-$d_6$): $\delta$ 341.99. Elem. Anal. Calcd. for $C_8H_4N_2Se_2$: C, 33.59; H, 1.41; N, 9.79. Found: C, 33.34; H, 1.57; N, 9.16. Crystals for X-ray diffraction were obtained as yellow rods from $CHCl_3$ solution by concentration.

**Compound 3.** Yield: 60%. Yellow solid, mp 148–153 °C. $^1$H NMR (300 MHz, DMSO-$d_6$): $\delta$ 7.49 (s, 4H). $^{13}$C NMR (75 MHz, DMSO-$d_6$): $\delta$ 138.61, 124.49, 105.94. $^{77}$Se NMR (76 MHz, DMSO-$d_6$): $\delta$ 273.47. Elem. Anal. Calcd. for $C_6H_2N_2SSe_2$: C, 24.67; H, 0.69; N, 9.59; S, 10.98. Found: C, 25.05; H, 0.85; N, 9.04; S, 11.15. Crystals for X-ray diffraction were obtained as yellow rods after dissolution in small amount of hot AcOEt and slow cooling to +5 °C.

**Compound 4.** Yield: 73%. Pale yellow solid, mp 156–158 °C (reported 156°).[12c] $^1$H NMR (300 MHz, DMSO-$d_6$): $\delta$ 7.77 (s, 4H). $^{13}$C NMR (75 MHz, DMSO-$d_6$): $\delta$ 134.84, 126.23, 105.49. $^{77}$Se NMR (76 MHz, DMSO-$d_6$): $\delta$ 334.46. Elem. Anal. Calcd. for $C_8H_4N_2Se_2$: C, 33.59; H, 1.41; N, 9.79. Found: C, 34.01; H, 1.51; N, 9.55. Crystals for X-ray diffraction were obtained as yellow rods after dissolution in small amount of hot AcOEt and slow cooling to RT and layering with petroleum ether.

### Co-crystallization experiments with bpen

With **2**: in a test tube, 14 mg (0.05 mmol) of **2** and 9 mg (0.05 mmol) of **bpen** were dissolved in 0.5 ml of $CHCl_3$. On top of the solution, pentane was added slowly to prevent mixing of the solvents and the test tube was sealed. After three days yellow crystals appeared (mp 81–82 °C). Elemental analysis was hampered by the systematic presence of starting materials co-precipitating with the product.

With **4**: in a test tube, 14 mg (0.05 mmol) of **4** and 9 mg (0.05 mmol) of **bpen** were dissolved in 1 ml of acetonitrile and left for slow evaporation of the solvent. After three days light brown crystals appeared (mp 188–190 °C). Elem. Anal. Calcd. for $(C_8H_4N_2Se_2)\cdot(C_{12}H_{10}N_2)$: C, 51.30; H, 3.01; N, 11.96 found: C, 51.36; H, 2.81; N, 11.86.

**Crystallography.** Data collections at RT were performed on an APEXII Bruker-AXS diffractometer equipped with a CCD camera and data collections at 150 K on a D8 VENTURE Bruker AXS diffractometer. Structures were solved by direct methods using the *SIR97* program,[22] and then refined with full-matrix least-square methods based on $F^2$ (*SHELXL-2014/7*)[23] with the aid of the *WINGX* program.[24] All non-hydrogen atoms were refined with anisotropic atomic displacement parameters. H atoms were finally included in their calculated positions. Details about data collection and solution refinement are given in Table S1.† The crystallographic data for all compounds were deposited in the Cambridge Crystallographic Data Centre (CCDC) with the CCDC no. 2280515–2280520.

## Conflicts of interest

There are no conflicts to declare.

## Acknowledgements

We thank ANR (Paris) for financial support under grant ANR-17-CE07-0025-02. This work has been also supported by the Integrated Development Program of the Gdańsk University of Technology program No. POWR.03.05.00-00.Z044/17 funded by the European Social Fund under the Knowledge Education Development Operational Program. Computations were carried out using the computers of Centre of Informatics Tricity Academic Supercomputer & Network.

## Notes and references

1 P. Metrangolo and G. Resnati, *Chem. – Eur. J.*, 2001, **7**, 2511–2519.
2 P. Metrangolo, H. Neukirch, T. Pilati and G. Resnati, *Acc. Chem. Res.*, 2005, **38**, 386–395.
3 G. Cavallo, P. Metrangolo, T. Pilati, G. Resnati and G. Terraneo, *Cryst. Growth Des.*, 2014, **14**, 2697–2702.
4 (*a*) D. B. Werz, R. Gleiter and F. Rominger, *J. Am. Chem. Soc.*, 2002, **124**, 10638–10639; (*b*) J. S. Murray, P. Lane, T. Clark and P. Politzer, *J. Mol. Model.*, 2007, **13**, 1033–1038.
5 E. Arunan, G. R. Desiraju, R. A. Klein, J. Sadlej, S. Scheiner, I. Alkorta, D. C. Clary, R. H. Crabtree, J. J. Dannenberg, P. Hobza, H. G. Kjaergaard, A. C. Legon, B. Mennucci and D. J. Nesbitt, *Pure Appl. Chem.*, 2011, **83**, 1637–1641.
6 (*a*) L. Vogel, P. Wonner and S. M. Huber, *Angew. Chem., Int. Ed.*, 2019, **58**, 1880–1891; (*b*) K. T. Mahmudov, M. N.

 

Kopylovich, M. F. C. Guedes da Silva and A. J. L. Pombeiro, *Dalton Trans.*, 2017, **46**, 10121–10138; (*c*) M. Fourmigué and A. Dhaka, *Coord. Chem. Rev.*, 2020, **403**, 213084; (*d*) N. Biot and D. Bonifaci, *Coord. Chem. Rev.*, 2020, **413**, 213243; (*e*) L. Brammer, A. Peuronen and T. M. Rosevaere, *Acta Crystallogr., Sect. C: Struct. Chem.*, 2023, **79**, 204–216.

7 (*a*) P. C. Ho, P. Szydlowski, J. Sinclair, P. J. W. Elder, J. Kubel, C. Gendy, L. M. Lee, H. Jenkins, J. F. Britten, D. R. Morim and I. Vargas-Baca, *Nat. Commun.*, 2016, **7**, 11299; (*b*) J. Kübel, P. J. W. Elder, H. A. Jenkins and I. Vargas-Baca, *Dalton Trans.*, 2010, **39**, 11126–11128.

8 (*a*) A. F. Cozzolino, Q. Yang and I. Vargas-Baca, *Cryst. Growth Des.*, 2010, **10**, 4959–4964; (*b*) A. F. Cozzolino and I. Vargas-Baca, *J. Organomet. Chem.*, 2007, **692**, 2654–2657.

9 A. Kremer, A. Fermi, N. Biot, J. Wouters and D. Bonifazi, *Chem. – Eur. J.*, 2016, **22**, 5665–5675.

10 O. Jeannin, H.-T. Huynh, A. M. S. Riel and M. Fourmigué, *New J. Chem.*, 2018, **42**, 10502–10509.

11 (*a*) H.-T. Huynh, O. Jeannin and M. Fourmigué, *Chem. Commun.*, 2017, **53**, 8467–8469; (*b*) K. Maartmann-Moe, K. A. Sanderud and J. Songstad, *Acta Chem. Scand., Ser. A*, 1984, **38**, 187–200; (*c*) S. L. W. McWhinnie, A. B. Brooks and I. Abrahams, *Acta Crystallogr., Sect. C: Cryst. Struct. Commun.*, 1998, **54**, 126–128; (*d*) A. Lari, R. Gleiter and F. Rominger, *Eur. J. Org. Chem.*, 2009, 2267–2274; (*e*) A. M. S. Riel, O. Jeannin, O. B. Berryman and M. Fourmigué, *Acta Crystallogr., Sect. B: Struct. Sci., Cryst. Eng. Mater.*, 2019, **75**, 34–38; (*f*) H.-T. Huynh, O. Jeannin and M. Fourmigué, *New J. Chem.*, 2021, **45**, 76–84; (*g*) A. M. S. Riel, H.-T. Huynh, O. Jeannin, O. Berryman and M. Fourmigué, *Cryst. Growth Des.*, 2019, **19**, 1418–1425.

12 (*a*) N. A. Barnes, S. M. Godfrey, R. T. A. Halton, I. Mushtaq, S. Parsons, R. G. Pritchard and M. Sadler, *Polyhedron*, 2007, **26**, 1053–1060; (*b*) T. M. Klapötke, B. Krumm and K. Polborn, *Eur. J. Inorg. Chem.*, 1999, 1359–1366; (*c*) W. S. McDonald and L. D. Pettit, *J. Chem. Soc. A*, 1970, 2044–2046; (*d*) T. M. Klapötke, B. Krumm, P. Mayer, H. Piotrowski and M. Vogt, *Z. Anorg. Allg. Chem.*, 2003, **629**, 1117–1123.

13 J. Alfuth, O. Jeannin and M. Fourmigué, *Angew. Chem., Int. Ed.*, 2022, **61**, e202206249.

14 P. Nikolaienko and M. Rueping, *Chem. – Eur. J.*, 2016, **22**, 2620–2623.

15 Y. Guan and S. D. Townsend, *Org. Lett.*, 2017, **19**, 5252–5255.

16 W. H. H. Guenther and M. N. Salzman, *Ann. N. Y. Acad. Sci.*, 1972, **192**, 25–43.

17 X. Zhang, X.-B. Huang, Y.-B. Zhou, M.-C. Liu and H.-Y. Wu, *Chem. – Eur. J.*, 2021, **27**, 944–948.

18 S. Redon, A. R. O. Kosso, J. Broggi and P. Vanelle, *Synthesis*, 2019, **51**, 3758–3765.

19 (*a*) K. Durka, K. N. Jarzembska, R. Kaminski, S. Lulinski, J. Serwatowski and K. Wozniak, *Cryst. Growth Des.*, 2013, **13**, 4181–4185; (*b*) O. Seven, M. Bolte, H.-W. Lerner and M. Wagner, *Organometallics*, 2014, **33**, 1291–1299.

20 H. Wang, J. Liu and W. Wang, *Phys. Chem. Chem. Phys.*, 2018, **20**, 5227–5234.

21 J. Cui, M. Wei, L. Pang, J. Xiao, C. Gan, J. Guo, C. Xie, Q. Zhu and Y. Huang, *Tetrahedron*, 2020, **76**, 130978.

22 A. Altomare, M. C. Burla, M. Camalli, G. Cascarano, C. Giacovazzo, A. Guagliardi, A. G. G. Moliterni, G. Polidori and R. Spagna, *J. Appl. Crystallogr.*, 1999, **32**, 115–119.

23 G. M. Sheldrick, *Acta Crystallogr., Sect. C: Struct. Chem.*, 2015, **71**, 3–8.

24 L. G. Farrugia, *J. Appl. Crystallogr.*, 2012, **45**, 849–854.